An ECG Acquisition System Prototype Design With Flexible PDMS Dry Electrodes and Variable Transform Length DCT-IV Based Compression Algorithm

Ching-Hsing Luo, Wei-Jhe Ma, Wen-Ho Juang, Shin-Hung Kuo, Chih-Yuan Chen, Pei-Chen Tai, and Shin-Chi Lai

***Abstract*— In this paper, a system is designed using flexible poly-dimethylsiloxane (PDMS) dry electrodes instead of wet electrodes to acquire electrocardiogram (ECG) signals. This flexible PDMS dry electrode (FPDE) is revised from the hard commercial biopotential conductive snap to a flexible electrode using a replica method that provides a reliable attachment for the ECG measurement method. The measurement result shows the proposed FPDE, which has the ability to acquire ECG signals, is comparable with the traditional wet electrodes applied in medicine. In addition, an acquisition circuit design integrated with commercial ICs and an field-programmable gate array (FPGA) platform is built for the development of long-term ECG monitoring. A variable-transform-length DCT-IV-based ECG compression algorithm with a higher quality score (QS) and a better compressing ratio (CR) is further proposed to significantly reduce the large amount of recording data in both storage and transmission. The QS parameter, which denotes a ratio of a CR value to a percent rms difference (PRD) value, is another key index applied to fairly evaluate the performance of various compression algorithms. DCT-IV is used as a unified transform kernel for ECG signal encoding and decoding, because the forward DCT-IV formula is the same as its inverse. It can be easily converted into a compact hardware accelerator with fewer hardware resources. To fairly evaluate the proposed compression algorithm, ECG signals sourced from MIT-BIT arrhythmia database with a sampling rate of 360 Hz are employed as the test patterns. The simulation results show the averages of CR, PRD, and QS to be 6.86, 0.18, 2.60, 1.68, 32.19, and 39.86, respectively, for all 48 lead-II patterns of the MIT-BIH database. Compared with Lee *et al.*'s DCT-II based algorithm, the QS value of the proposed method exhibits a 76% improvement. The experimental results clearly show that the proposed system would be a better choice for achieving ECG signal acquisition in the future.**

Manuscript received March 6, 2016; revised June 6, 2016; accepted June 22, 2016. Date of publication June 28, 2016; date of current version November 4, 2016. This work was also supported in part by the National Science Council, Taiwan under Grant 101-2218-E-006-005 and Grant 101-2221-E-006-271. The associate editor coordinating the review of this paper and approving it for publication was Prof. Daniela De Venuto. *(Corresponding author: Shin-Chi Lai.)*

C.-H. Luo, W.-J. Ma, W.-H. Juang, S.-H. Kuo, C.-Y. Chen, and P.-C. Tai are with the Department of Electrical Engineering, National Cheng Kung University, Tainan 70101, Taiwan (e-mail: robin@ee.ncku.edu.tw; harukokashi@gmail.com; riverjuang@gmail.com; guosuicune@gmail.com; chen0207@gmail.com; cl34041442@gmail.com).

S.-C. Lai is with the Department of Computer Science and Information Engineering, Nanhua University, Chiayi 62249, Taiwan (e-mail: shivan0111@nhu.edu.tw).

Digital Object Identifier 10.1109/JSEN.2016.2584648

***Index Terms*— Dry electrode, lossy compression, electrocardiogram (ECG), the type-IV of discrete cosine transform (DCT-IV), poly-dimethylsiloxane (PDMS).**

I. Introduction

RECENTLY, monitoring the physiology of patients and personal health care has been integrated in modern wireless e-health systems. This is essential for long time monitoring or to obtain 24-hr nonstop recordings in the case of electrocardiogram (ECG), electroencephalogram (EEG), and various other bio-signals. The electrodes used for signal acquisition directly affect the quality of the biomedical signal. One of the significant issues in measuring ECG signals is how to comfortably detect these using dry electrodes in lieu of wet electrodes. This is because wet electrodes contact and cover the skin through the use of an electrolyte gel, which causes itchiness, reddening and swelling. Bio-potential electrodes can transform signals from the skin tissue to the acquisition device. Bio-electrodes (e.g., wet electrodes) have traditionally been used to record bio-potential signals by using electric gels that improve electric conductivity. While these gel substances can fix the electrode on the skin, they can also provoke dermal irritation and even allergies. Furthermore, the conductivity of electrolytic gel decreases gradually due to hardening, subsequently degrading the data acquisition quality. Therefore, exploiting the use of various materials for the purpose of fabricating bio-compatible electrodes is worth consideration.

In recent years a great deal of attention has been focused on dry electrodes [1]–[9] designs that are operated without electrolyte gel and skin preparation, such as Micro-Electro-Mechanical-Systems (MEMS) dry electrodes (intrusive) [1]–[7], and soft dry electrodes (nonintrusive) [8]. Another type of dry electrode was made using poly-dimethylsiloxane (PDMS) material [9], [33], which can fit the curved surface of the human body and do not damage the skin.

Since electrode sensors were discussed above, the design of acquisition system should also be considered. Recently, the ECG acquisition system literature has been paying increased attention to integration with low power acquisition chips [6], [7], [10], [11]. Moreover, a novel power

management method has been developed for a physiological signal acquisition device that can greatly reduce system power consumption [6]. Nemati *et al.*'s design [10] obtained long battery life by using low-power consumption components and developing battery-saving control techniques. Chang *et al.* [7] and Wang *et al.* [11] proposed an analog front-end circuit for bio-potential acquisition with low power consumption. These systems were composed of an instrumentation amplifier (IA), a band-pass filter, and a gain stage. Because noise interference with ECG signals will be coupled to the human body, front-end circuits with a high common mode rejection ratio (CMRR) and power supply rejection ratio (PSRR) are very important for signal acquisition. Power consumption is another critical issue for portable physiological acquisition systems. Based on previous studies, most of the power consumption involved in acquisition is caused by the radio frequency transceiver data transmission. This implies that a great amount of power could be saved if the transmitted data could be compressed. Long time monitoring results in a huge amount of information, and thus data compression would be useful not only for wireless data transmission, but also for data storage, especially when the physiological signals are acquired and utilized for medical diagnostic and health care purposes. As such, many approaches [12]–[19] were used to significantly reduce the memory space needed for storing medical recordings, shortening communication times and have lowering the power consumed by monitoring devices.

Gan *et al.* [12] proposed a design incorporating low-complexity ECG signal compression, and Chen *et al.* [13] also provided an adaptive power conserving algorithm and a data compressing method with a four-level hierarchical wireless body sensor network. This method is very suitable for low-power implementations of a physiological acquisition system, although it requires a small hardware overhead. The results showed compression rates for body temperature, pulse oxygen, and blood glucose signals of up to 3.33, and compression rates for blood pressure, ECG, and EEG signals of 1.92. This also demonstrates that the power consumption related to data transmission will be greatly reduced using such systems.

Generally speaking, compression methods are classified as either lossy or lossless. Lossy methods for compressing ECG signals has been widely used because of the high compression ratio performance. Previous research in this area can be divided into three categories [14]. The first computes the redundancy from the signals and then removes this to achieve a higher data compression ratio. The second is the transformation method [15]–[20], which converts a time domain signal into a frequency or other domains and compresses the spectral or energy components, such as FFT, DCT, DWT, and so on. The third is the parameter extraction compression method, which includes the peak picking method and the linear prediction method.

Alam and Rahim [16] proposed an improved transform method that achieves better CR and PRD metric results than those of Batista *et al.* [15]. The above-referenced algorithms perform quantization of the DCT transform. However, a common shortcoming of Batista *et al.* [15] and Alam and Rahim [16] is the inability to compute the algorithms in real time. This results in a long and costly time delay when executing the data compression of large amounts of ECG samples in the offline mode. Recently, Lee *et al.* [17], [18] proposed an efficient DCT-II-based algorithm for ECG compression, where the acquired N-point ECG signal is firstly downsampled by a factor of two. The downsampled sequence is then processed using a backward differential procedure to achieve a 75% reduction of original data. The processed samples between R-R intervals are then transformed using the DCT-II, and the fractional parts of the transformed coefficients are discarded to obtain the compressed bit stream using Huffman coding. Mukhopadyay *et al.* [21], [22] proposed another algorithm that converts the original signals into ASCII bits and compresses these bit streams using ASCII algorithms [23].

In contrast to the algorithms referenced above, this paper extends previous work [24] by proposing an effective ECG compression algorithm which can be run in real-time on any portable device to access and transmit bio-signals for a personal health system application. This algorithm analyzes the corresponding spectral and energy components of ECG samples through the DCT-IV frequency domain. The processed samples have smaller dynamic range characteristics as a result of using backward differential computation and non-uniform quantization to reduce the amount of representative sample data. An additional step is used for recording irregularly interleaved transformed coefficient sign bits after the DCT-IV procedure to further decrease the total number of data samples. The lossless Huffman encoding technique [25] is finally employed to obtain the compressed bit stream. Compared to the latest algorithms for compressing ECG samples, 48 instances in the MIT-BIH arrhythmia database [26] are used as the test samples for evaluation of the proposed algorithm in this work. In addition, we also implement a DCT-IV hardware accelerator to reduce the computational complexity of ECG compression in the algorithm. Here, we can utilize the nature of a recursive algorithm [27], [28] to obtain a small, compact DCT-IV structure, and then achieve a variable-transform-length DCT-IV application in the future.

The proposed design in this study focuses on the following topics: 1) the PDMS material is used to fabricate a sensor substrate through MEMS technology and replica methods. There is no damage to the skin, and it is more suitable for long-term wear than other alternatives; 2) the proposed system utilizes some commercial ICs as key components, such as a front-end circuit, an analog-to-digital (ADC) converter and digital signal processing circuits, using Altera FPGA. Additionally, a Nios2 processor is built for data control and task management. To shorten the time required for data compression and avoid overloading the Nios2 processor, a concept for both hardware and software co-design is employed to achieve a compression algorithm; 3) a new, efficient DCT-IV-based ECG compression algorithm with a higher QS and a better CR is developed and executed using a Nios2 processor. A fast recursive DCT-IV hardware accelerator is then implemented using Altera FPGA, and is integrated with Nios2 for the proposed ECG acquisition system.

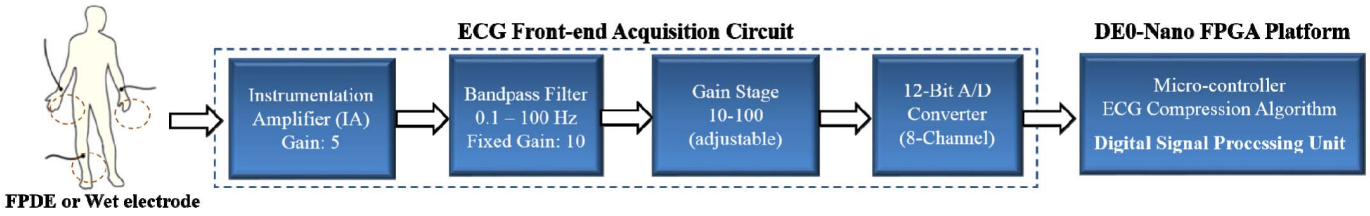

Fig. 1. Function blocks of the proposed ECG signal acquisition system.

The rest of this paper is organized as follows: Section II proposes a flexible PDMS dry electrode (FPDE) and ECG acquisition circuit design. Section III introduces a novel ECG compression algorithm and the proposed DCT-IV hardware accelerator. Section IV discusses the results of the FPDE performance analysis and shows the entire ECG acquisition system. Section V provides a detailed performance analysis for the proposed ECG compression algorithm, and compares the differences with a state-of-the-art approach. Finally, the conclusions of this work are given in Section VI.

II. Proposed Flexible PDMS Dry Electrode and ECG Acquisition Circuit Design

In this section, an FPDE with an acquisition circuit is applied for the purpose of measuring ECG signals without skin preparation or conductive gel usage. The function blocks of the proposed acquisition system, as shown in Fig.1, is comfortable and effective for ECG signal measurement, since it has been integrated with the DE0-nano FPGA platform, where some digital signal processing methods, such as the ECG compression algorithm, can be developed.

A. Flexible PDMS Dry Electrode Fabrication Process

The quality of the biomedical signal is affected by using the relative acquisition electrodes. Some dry electrodes are made of stiff substrates that can damage skin tissue when the electrode is removed. Gruetzmann *et al.* [8] proposed a soft and flexible electrode to address the effects of motion artifacts in order to reduced contact impedance during ECG measurement. Under slight pressure, the soft and flexible dry electrodes on the skin better stabilize contact with the skin as compared to hard electrodes. Recently, soft electrodes made by PDMS have proven to be bio-compatible and are made of a durable material that does not damage human skin. In addition, a soft electrode can increase the contact area, which reduces contact impedance with the skin. A comparison of an electrode-skin interface standard wet electrode with other kinds of dry electrodes is shown in Fig. 2.

PDMS is widely used in various biomedical applications because of its flexibility and the fact that it is made of a good biocompatible material. Baek *et al.* was the first to propose a PDMS-based flexible dry electrode [9] for bio-potential measurement. Kim *et al.* [32] and Moon *et al.* [33] used same material to fabricate a sensor substrate using MEMS technology. However, connecting the wire to the PDMS electrode is challenging, and thus far conductive glue has been used as the connective interface between the wire and the PDMS surface.

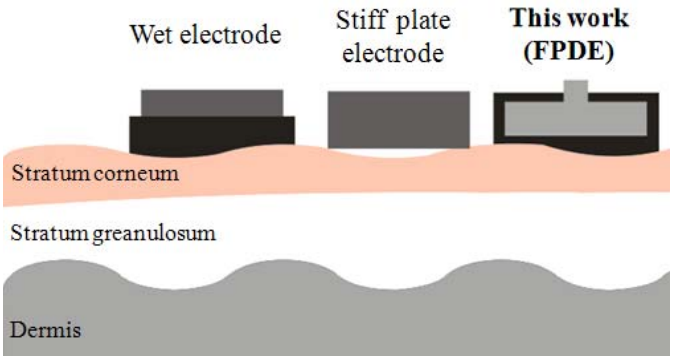

Fig. 2. Schematic of skin structures and different kinds of electrode penetration concepts.

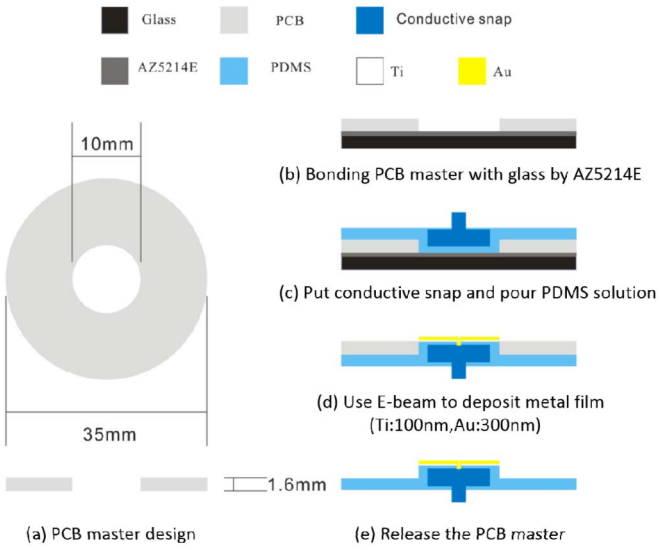

Fig. 3. PDMS molding process flow.

In this work, a new fabrication method is proposed that transforms a commercial bio-potential conductive snap (MEDI-TRACETM, COVIDIEN, USA) into an FPDE using a replica method. It provides a convenient wire connection method that produces a stable signal and can be combined with conventional hospital ECG measurement instruments. The FPDE structure was fabricated using 35 × 35 mm2 printed circuit board (PCB), with a commercial circuit board plotter machine (ProtoMat C40, LPKF Laser & Electronics, North America) has been used. First, the circle was fixed on one side as a master by using ProtoMat C40. After the master was finished, it was cleaned using deionized (DI) water and acetone, and the ProtoMat C40 was used to drill the master design. The PCB master has two main uses: (1) an FPDE

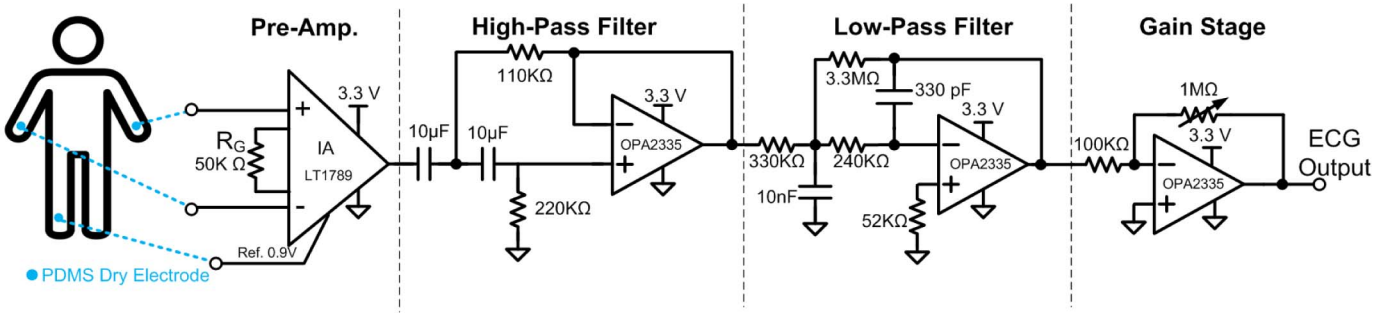

Fig. 4. The proposed front-end signal acquisition circuit.

structural definition, and (2) a metal deposition definition. This technique was applied to fabricate the FPDE, and universal electrode manufacturing methods are used that employ photolithography and metal etching processes. The proposed method fabricates a high aspect ratio 3D structure and can define a metal pattern on the PDMS surface, greatly reducing metal etching and environmental pollution. Since the PCB master can be reused, production time is also reduced. The PDMS solution in this work was prepared from a mixture of a Sylgard 184 silicon elastomer base and a silicon elastomer curing agent (from Dow Corning) with a weight ratio of 10:1. After mixing, the PDMS was placed into a vacuum chamber at 750 mmHg for 30 minutes to eliminate air bubbles. The PDMS solution was poured into the master and cured at 85° C for 1 hour. After curing, the PDMS structure was peeled off the master. On the PDMS surface, we used a biopsy punch and deposited Ti (100nm) and Au (300nm) metal by E-beam evaporation [29]. The PDMS replica molding process when using the master is shown in Fig. 3.

B. Front-End Signal Acquisition Circuit Design

An acquisition circuit was proposed in this paper to measure ECG signals. An instrumentation amplifier (LT1789, Linear Technology Corporation) was used as the pre-amplifier for the purpose of sensing ECG signals in the circuit. LT1789 has a number of advantages, including high CMRR, high PSRR, high accuracy, and a rail-to-rail input and output range. Some environmental noise can be cancelled with a high-input-impedance and high CMRR commercial IA. In order to amplify the input ECG signals to the desired amplitude, the gain needs to be adjusted (2000∼3000 V/V), and a band-pass filter (0.1–100Hz) is designed for the ECG acquisition. Additionally, the proposed front-end signal acquisition circuit could be powered by a rechargeable 3.7V battery. A schematic view of the front-end circuit is shown in Fig. 4, and the related parameters of all elements are also given in detail. The proposed pre-amplifier provides a DC gain of 5 V/V; the frequency ranges of the proposed band-pass filter, which consists of a high-pass filter and a low-pass filter, is from 0.1 to 100 Hz, and the gain stage provides a maximum DC gain of 100 V/V.

C. DE0-Nano FPGA Platform within Nios2 Processor and Analog-to-Digital Converter

In the proposed design, we utilize the DE0-nano FPGA platform to create a Nios2 processor and a compact

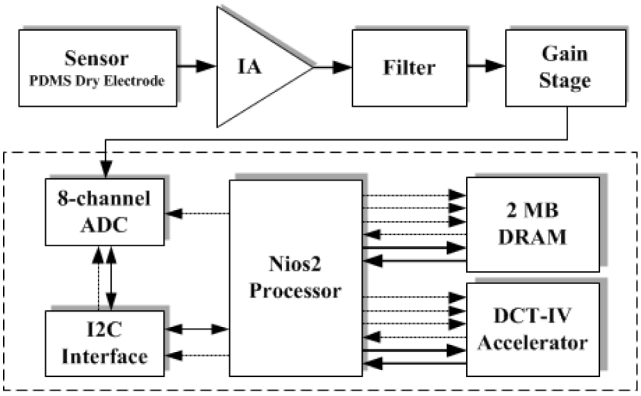

Fig. 5. Functional blocks of the proposed front-end circuit and a DSP unit based on Altera DE0-Nano platform.

DCT-IV hardware accelerator. The Nios2 processor can be easily created using an SOPC builder in Quartus2 software for an Altera FPGA device. It can be treated as a powerful Digital Signal Processing (DSP) unit, where programmers can use C/C++ language to develop some programs and functions on the processor. Since the Nios2 processor and the DCT-IV accelerator are both composed of FPGAs, the structure is reconfigurable, which creates a huge advantage related to flexibility with respect to functional usage and algorithm development. This also implies that we can develop the proposed ECG compression algorithm by using a hardware and software co-design concept. Figure 5 demonstrates the functional blocks of the proposed DSP unit with 2 Mega-Bytes DRAM and 8-channel 12-bits ADC on the FPGA platform. Therefore, it is an extremely compact, useful, and powerful development board, especially suited to ECG compression or biomedical signal processing.

III. Proposed ECG Compression Algorithm and Its Hardware Accelerator Design

As shown in Fig. 6(b), there are a total of eight processing procedures for ECG data compression and decompression. The original ECG signal is sampled by an ADC first and then is sent to the Nios2 processor through the I^2C interface. The details are introduced as follows:

A. 1/2 Downsampling and Normalization

In this work, the ECG signal from the MIT-BIH database is employed for algorithm development. The sampling rate

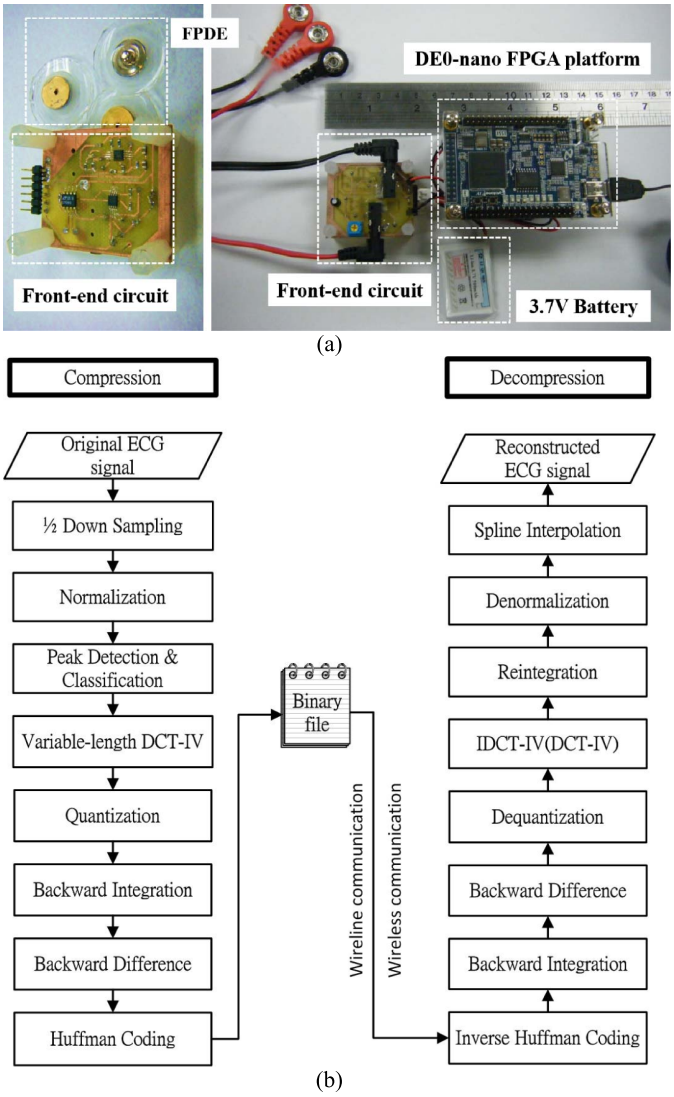

Fig. 6. Block diagram of the proposed ECG acquisition design. (a) Block diagram of the proposed ECG acquisition system. (b) Block diagram of the compression and decompression procedures.

of each 11-bit ECG signal is 360 Hz and then restore as two bytes to temporal data. After the 1/2 downsampling process is completed, a 50% reduction in total data can be easily achieved. However, the reconstructed ECG signal loses a little accuracy in order to obtain this benefit. The ECG signal, which ranges from 0 to 2047, is normalized by dividing a factor of the maximum input data, i.e. 2048. The dynamic range of the normalized ECG signal ranges from 0 to 1. The normalization formula is shown as (1).

$$Normalized\ Signal = \frac{OriginalSignal}{2048} \tag{1}$$

$$Threshold = \begin{cases} avg(X5[1 : i + 100]), \\ \qquad i = 1 \sim 100; \\ avg(X5[i - 100 : i + 100]), \\ \qquad i = 101 \sim (\text{TotalLength} - 100); \\ avg(X5[i - 100 : \text{TotalLength}]), \\ \qquad i = (\text{TotalLength} - 100) \sim \text{TotalLength}; \end{cases} \tag{2}$$

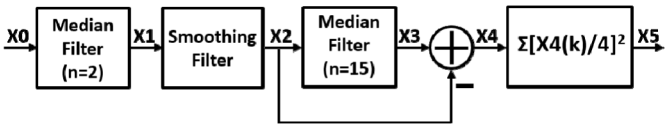

Fig. 7. Computational flowchart of the pre-processing stage.

B. Peak Detection and Segmentation

The peak detection (PD) algorithm is applied to segment the ECG signal into a repeating and time-interval signal. This method is useful for R-wave signal location under each time interval. In the proposed method, there are two main stages, i.e. pre-processing and decision stages, in the PD algorithm. The first one uses a 2-order median filter and a smoothing filter. Then a 15-order median filter and average computation are both required. The computational flowchart of this pre-processing stage and its corresponding waveform are shown in Fig. 7 and Fig. 8, respectively. First, the X0 waveform, as shown in Fig. 8(a), uses a 2-order recursive median filter to lower the magnitude of R-wave and T-wave. Figure 8(b) shows that the signal of X1 after the median filter has a lower magnitude. Second, the X1 waveform further uses a smoothing filter, as shown in Fig. 8(c), to generate the X2 waveform, which also retains the trend of the X0 waveform. Third, the X3 waveform, as shown in Fig. 8(d), is the result of X2 passing through a 15-order median filter. Fourth, the X3 waveform retains most of the T-wave, but eliminates a part of R-wave compared with the X2 waveform. Fifth, the X4 waveform, as shown in Fig. 8(e), used the X3 waveform to subtract the X2 waveform, and then the locations of the T-wave and R-wave can be efficiently eliminated. After taking the square and avenge operations for the X4 waveform, the results of the pre-processing stage are shown in Fig. 8(f). Finally, a threshold calculation formula (2) is employed in the decision stage. Since the X5 waveform, as shown in Fig. 8(f), is regular, we can easily recognize the first greater peak to be the R-wave location. All the magnitude values on the y-axis of Fig. 8(a) to Fig. 8(f) are digitized quantization values sampled by 11-bit ADC according to the MIT-BIH database. To make sure that the R-R interval (RRI) is limited to 512 samples, a cutting segment computational flow is shown in Fig. 9.

C. Variable-Transform-Length DCT-IV Computation and Uniform Quantization

An N-point DCT-IV formula is defined as (3), where x[n] and X[k] are, respectively, time-domain sequence and frequency-domain coefficients.

$$X[k] = \sqrt{\frac{2}{N}} \times \sum_{n=0}^{N-1} x[n] \times \cos\left((2n+1)(2k+1)\pi/(4N)\right), \quad where\ k\ is\ 0\ to\ N-1. \tag{3}$$

By exchanging indices n and k, it can be easily proven that the inverse of the DCT-IV is the same as the DCT-IV. Figure 10 shows that the instance (record #100, sampling index from 1 to 64) transformed by DCT-IV has two particular characteristics. First, the DCT-IV spectrum converges to zero with increases in the coefficient index. Second, the amplitude sign bit repeats regularly according to the following

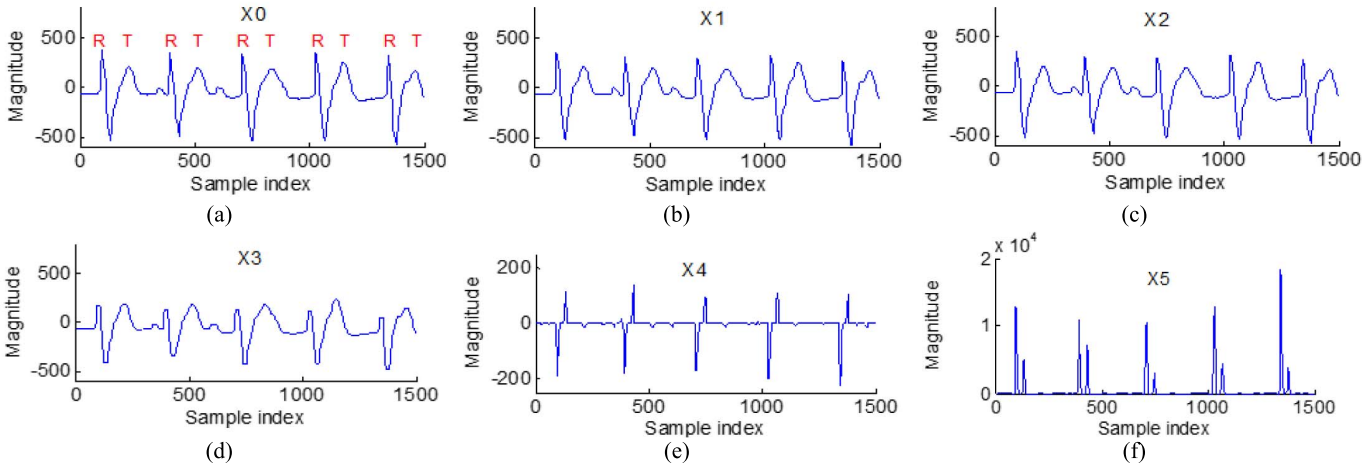

Fig. 8. The waveform of the pre-processing stage: (a) X0 waveform; (b) X1 waveform (after 2-order median filter); (c) X2 waveform (after smoothing filter); (d) X3 waveform (after15-order median filter); (e) X4 waveform (after subtraction of X2 from X3); and (f) X5 waveform (after taking square and avenge operations).

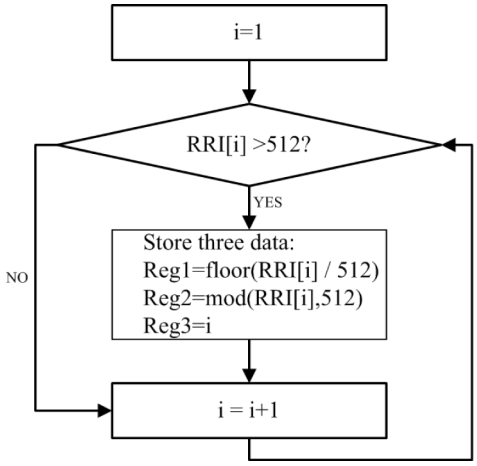

Fig. 9. Computational flowchart of the cutting segment.

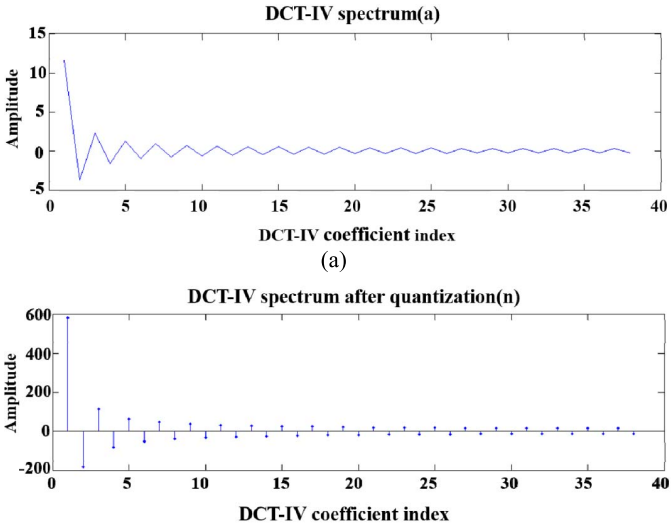

Fig. 10. The characteristics of the DCT-IV spectrum. (a) DCT-IV spectrum (record no.100, where the data indices are from 39 to 185). (b) DCT-IV spectrum after quantization.

rule, i.e. −, +, ..., −, and +, although the amplitude exhibits a slightly unstable rise from coefficient index#1 to coefficient index#30. Here, we propose a method to separate the amplitude into one sign symbol (1 bit) and magnitude (floating point). It can be easily found that the magnitudes between each index of the DCT-IV coefficients are very close to each other, and this characteristic can be applied to combine with the backward differential computation to generate a new sequence. After we obtain the spectrum sequence, the uniform quantization procedure can be done. It can be observed from Fig. 10 that the magnitude of the DCT-IV coefficients will become very small when the index number is larger than 20. Each quantitative data unit is represented as an 11-bit sequence with a quantization number of 0.02. For the hardware accelerator design, an N-point DCT-IV algorithm neglecting the scaled factor is defined as

$$out[k] = \sum_{n=0}^{N-1} in[n] \times \cos\left((2n+1)(2k+1)\pi/(4N)\right) = \sum_{n=0}^{N-1} x[n] \times C_{k,n},$$

$$where\ C_{k,n} = \cos\left(\frac{\theta_k}{2} + n\theta_k\right),\ and\ \theta_k = \left(\frac{2k+1}{2}\right)\frac{\pi}{N} \quad (4)$$

After expressing the cosine function as a recursive form (5), we obtain a compact structure of the DCT-IV algorithm as shown in Fig. 11. The initial condition is defined as (6).

$$F_{c,n} = 2\cos\theta_k F_{c,n-1} - F_{c,n-2} \quad (5)$$

$$F_{c,0} = F_{c,-1} = \cos\left(\frac{\theta_k}{2}\right) \quad (6)$$

For the variable-transform-length DCT computation, an on-line cosine coefficient generator and an accumulator are designed, as shown in Fig. 11. The input sequence should be multiplied by a cosine coefficient in every clock, and then the results are fed into the accumulators to calculate the desired DCT-IV coefficients. It is clearly seen that the proposed DCT-IV accelerator requires three registers, two adders, and

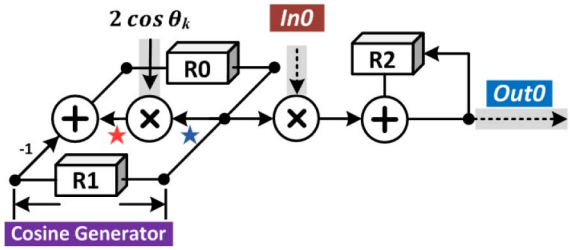

Fig. 11. Proposed Compact DCT-IV Accelerator Design.

TABLE I
PROPOSED HUFFMAN TABLE AND HUFFMAN TREE

Diff. Bit	Diff. Data		Occurring Prob.	Huffman Tree
0	0		0.31	[0,0]
1	-1	1	0.28	[0,1]
2	-3,-2	2,3	0.15	[1,0,0]
3	-7~-4	4~7	0.09	[1,1,0]
4	-15~-8	8~15	0.06	[1,0,1,0]
5	-31~-16	16~31	0.04	[1,1,1,0]
6	-63~-32	32~63	0.02	[1,0,1,1,0]
7	-127~-64	127~64	0.01	[1,1,1,1,0]
8	-255~-128	128~255	0.01	[1,0,1,1,1,1]
9	-511~-256	256~511	0.01	[1,1,1,1,1,1]
10	-1023~-512	512~1023	0.01	[1,0,1,1,1,0,0]
11	-2047~-1024	1024~2047	0.01	[1,1,1,1,1,0]
12	-4095~-2048	4095~2048	0.00	[1,0,1,1,1,0,1,0]
13	-8191~-4096	8191~4096	0.00	[1,0,1,1,1,0,1,1,0]
14	-16383~-8192	8192~16383	0.00	[1,0,1,1,1,0,1,1,1]

two multipliers. The FPGA implementation results show that the proposed DCT-IV hardware accelerator only uses 571 logic elements, 533 combinational functions, 160 logic registers and 16 multiplier 9-bit elements.

D. Backward Computation and Huffman Encoding

Since the DCT-IV spectrum has a strong and regular oscillation, we can use the following steps, including backward integration (4) and backward difference (5), for the purpose of shortening the coming sequence. The output sequence can thus be fed into the final procedure.

$$BI_Q = \begin{cases} Sq[1] = FreqQ[1] & if\ k = 1 \\ Sq[k] = FreqQ[k] + FreqQ[k-1], & if\ k \neq 1 \end{cases} \tag{7}$$

$$BD_Q = \begin{cases} Sq[1] = BI_Q[1] & if\ k = 1 \\ Sq[k] = BI_Q[k] - BI_Q[k-1], & if\ k \neq 1 \end{cases} \tag{8}$$

The final procedure of the proposed compression is entropy coding (also called Huffman coding). In this work, we adopt a concept similar to the JPEG [25] composed of one differential table and one Huffman table. After we simulated all of the ECG patterns in MIT-BIH database, we were able to specify the Huffman tree according to different occurring probabilities. Theoretically, the frequently occurring data would be allocated lower bits. The result shows that the proposed algorithm can achieve a better compression ratio. Table I shows the proposed Huffman table.

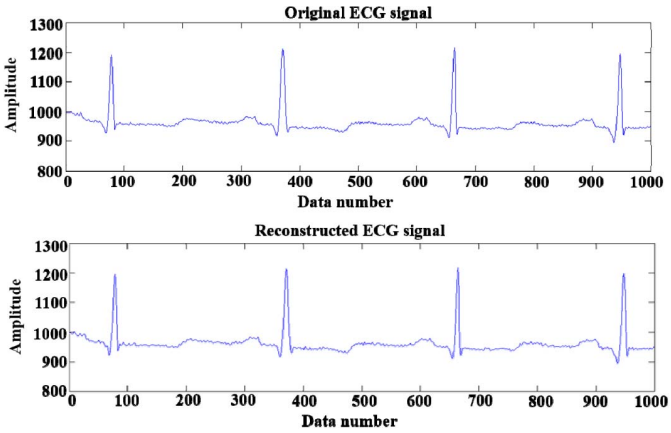

Fig. 12. Original ECG signal and its reconstruction after the proposed compression algorithm (MIT-BIH record no.100).

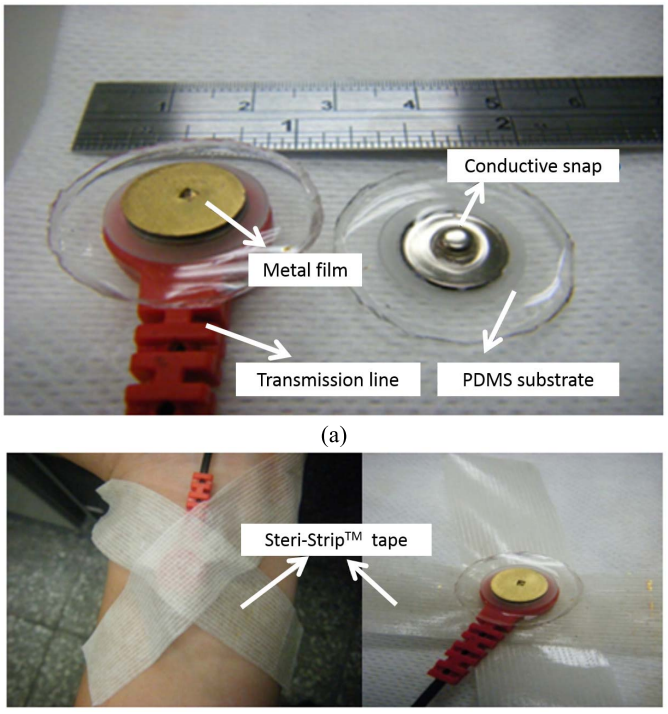

Fig. 13. (a) Proposed FPDE. (b) The FPDE placed on skin for measurements and the FPDE package.

E. Reconstruction of the Compressed ECG Data

The reconstruction of the compressed ECG signal is achieved using the reverse procedures from those on the right side of Fig. 6. The results show that the compressed bit-stream is well received and perfectly reconstructed using the proposed decompression. Figure 12 shows that the reconstruction of the ECG signal is quite similar to that of the original ECG signal.

IV. PERFORMANCE TESTS FOR THE PROPOSED FPDE AND ECG ACQUISITION SYSTEM

A. Proposed FPDE package

The FPDE is fabricated using a replica method. Ti (100nm) and Au (300nm) films are deposited stably on the PDMS surface, and the metal patterns are created through the use of a PCB mask, as described in Fig. 13(a). The metal film

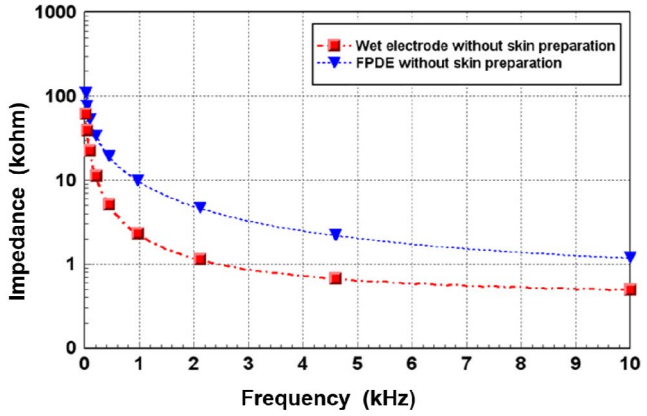

Fig. 14. Impedance measurement result for the proposed FPDE.

is uniformly deposited on the structure, and the area is about 78.5 mm^2. The PDMS electrode makes it easy and convenient to measure ECG signals, and Steri-StripTM (3M Company, U.S.A) tape is used to fix the FPDE on the skin, as shown in Fig. 13(b).

B. Measurement Results for the FPDE impedance

The impedance versus frequency measurement of the FPDE and the wet electrode are shown in Fig. 14. The precision LCR meter (Agilent E4980A precision LCR meter) is adopted for measuring both the FPDE and wet electrode impedances. The impedance analyzer can support the impedance measurement of two terminal components, such as capacitors, inductors, or resistors [30]. The wet electrode and the proposed FPDE are both placed on the forearm with a separation of 10cm, center to center, and then a voltage is applied to the electrode pair to measure the impedance changes. To guarantee reliable and reproducible results, the test signal for the impedance is set at 5mV, with the frequency ranging from 20 Hz to 10 kHz. Ten tests are performed on five different subjects, and the impedance value of the FPDE is similar to that of the wet electrode under the biomedical frequency band [9], [31].

C. Measurement Results for Medical Wet Electrode and the Proposed Flexible PDMS

The measured ECG data are transmitted to the DE0-nano FPGA platform using an I^{2}C bus. The size of the front-end acquisition circuit is 38×39 mm^2 in Fig.6 (a), and the device is powered by a single 3.7V battery power supply. For the ECG acquisition experiment, the proposed front-end circuit is combined with a medical wet electrode and the proposed flexible PDMS, respectively. A digital storage oscilloscope, Agilent DSO-X 2012A, is then employed to record and to observe the analog output signal coming from the front-end circuit. The analog output signal is also transformed into a 12-bit digitized sequence using the proposed DSP unit, i.e. the DE0-nano platform. Figure 15 shows two experimental results from the same subject when using wet and dry electrodes.

The results clearly show that the detecting signal of the proposed dry electrode is comparable to that of the medical wet electrode under the same conditions. Additionally, the

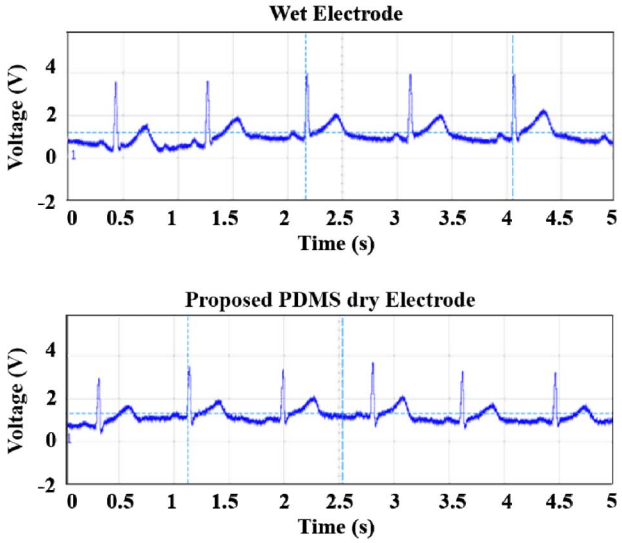

Fig. 15. ECG signal acquisition results for the wet electrode and the proposed FPDE using the Agilent oscilloscope.

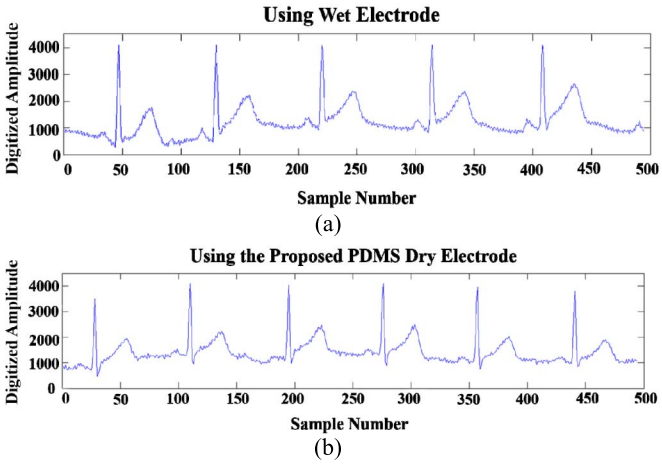

Fig. 16. ECG signal acquisition results for (a) wet electrode and (b) the proposed FPDE dry electrode using the proposed acquisition system.

proposed flexible PDMS will not lead to any itchiness or inflammation. Figure 16 presents the digitized signal corresponding to the one shown in Fig. 15, and the digitized quantization values shown on the y-axis are sampled by the 12-bit ADC of the proposed acquisition system. The top of Fig. 16(a) is for the wet electrode, and that of (b) is for the proposed dry electrode. Compared with Fig. 15, it can be found that the proposed ECG acquisition system can correctly convert the analog signals into digital data.

V. Performance Tests for Various ECG Compression Algorithms

In this section, six performance metrics from (9) to (15) are employed to evaluate the proposed ECG algorithms and other methods. These numerical measurements are, respectively, Compressing Ratio (CR), Root-mean-square (RMS), Percent RMS Difference (PRD), Percent RMS Difference Normalized (PDRN), Signal to Noise Ratio (SNR), and

TABLE II
PERFORMANCE RESULTS OF THE PROPOSED ALGORITHM

Pattern#	CR	PRD	PRDN	RMS	SNR	QS
100	7.78	0.18	4.41	1.70	27.11	44.00
101	7.98	0.17	3.12	1.63	30.11	47.40
102	5.90	0.17	4.35	1.66	27.23	34.71
103	7.89	0.17	2.62	1.69	31.63	45.81
104	5.71	0.22	4.35	2.18	27.22	25.65
105	7.09	0.18	2.19	1.78	33.17	39.15
106	6.91	0.18	2.45	1.80	32.22	37.98
107	4.93	0.16	0.93	1.59	40.65	30.70
108	5.98	0.14	2.46	1.41	32.18	41.62
109	7.32	0.18	1.76	1.76	35.08	40.91
111	6.36	0.14	2.69	1.39	31.39	45.34
112	6.26	0.14	2.50	1.25	32.03	43.25
113	7.82	0.22	2.61	2.16	31.65	36.13
114	6.01	0.14	4.40	1.41	27.14	42.26
115	7.88	0.19	2.47	1.79	32.16	40.86
116	7.11	0.28	1.81	2.40	34.86	25.11
117	6.12	0.17	3.00	1.47	30.46	35.57
118	7.05	0.22	2.17	1.86	33.28	32.56
119	7.26	0.20	1.63	1.75	35.75	35.67
121	7.16	0.14	2.10	1.25	33.54	49.44
122	7.50	0.22	2.59	1.90	31.72	33.93
123	8.18	0.19	2.82	1.64	30.98	43.22
124	8.08	0.17	1.63	1.50	35.78	46.66
200	5.71	0.15	2.01	1.53	33.92	37.52
201	6.76	0.13	3.30	1.28	29.63	52.49
202	7.35	0.17	2.78	1.65	31.13	44.15
203	5.94	0.19	1.94	1.93	34.23	30.67
205	7.21	0.16	4.04	1.59	27.88	43.77
207	6.28	0.14	1.97	1.39	34.10	44.68
208	6.63	0.18	1.88	1.81	34.51	36.40
209	6.59	0.19	3.59	1.93	28.90	33.98
210	7.01	0.17	3.32	1.73	29.58	40.19
212	6.92	0.20	2.94	1.95	30.64	35.36
213	6.76	0.18	1.35	1.81	37.39	36.89
214	7.03	0.18	1.86	1.75	34.59	39.94
215	5.41	0.16	2.77	1.56	31.16	34.50
217	5.97	0.17	1.37	1.69	37.25	35.24
219	7.80	0.18	1.49	1.65	36.52	43.27
220	7.71	0.23	3.31	2.11	29.60	33.55
221	7.02	0.17	2.85	1.72	30.89	40.64
222	5.88	0.15	3.88	1.44	28.22	40.51
223	7.10	0.18	2.01	1.63	33.95	40.21
228	6.05	0.15	2.10	1.46	33.54	41.45
230	7.47	0.17	2.32	1.65	32.67	45.01
231	8.27	0.15	2.76	1.50	31.17	54.67
232	6.23	0.12	3.74	1.23	28.55	50.24
233	6.41	0.17	1.55	1.68	36.21	38.08
234	7.37	0.18	2.60	1.76	31.69	41.73
Average	**6.86**	**0.18**	**2.60**	**1.68**	**32.19**	**39.86**

Quality Score (QS), which can be obtained as follows.

$$CR = \frac{Number of Original Data Bits}{Number of Compressed Data Bits}, \tag{9}$$

$$PRD(\%) = 100 \times \sqrt{\frac{\sum_{n=0}^{N-1}[X_s(n) - X_r(n)]^2}{\sum_{n=0}^{N-1} X_s(n)^2}}, \tag{10}$$

$$PRD\_wb(\%) = 100 \times \sqrt{\frac{\sum_{n=0}^{N-1}[X_s(n) - X_r(n)]^2}{\sum_{n=0}^{N-1}[X_s(n) - 1024]^2}}, \tag{11}$$

TABLE III
PERFORMANCE COMPARISON RESULTS OF THE PROPOSED ALGORITHM AND SOME RELATED APPROACHES

Method	CR	PRD	PRDN	RMS	SNR	QS
[16]	6.11*	0.78	unlisted	unlisted	unlisted	7.83
[18]	5.19	0.23	3.56	2.22	29.67	22.56
[19]	5.82*	0.80	unlisted	unlisted	unlisted	7.27
[20]	4.32	3.45	unlisted	unlisted	unlisted	1.25
[24]	5.26	0.19	3.66	1.84	30.10	28.08
Proposed	**6.86**	**0.18**	**2.60**	**1.68**	**32.19**	**39.86**

*has been adjusted to the same scale (from 11 bits to 16 bits)

$$PRDN(\%) = 100 \times \sqrt{\frac{\sum_{n=0}^{N-1}[X_s(n) - X_r(n)]^2}{\sum_{n=0}^{N-1}[X_s(n) - X_m]^2}}, \tag{12}$$

$$RMS = \sqrt{\frac{\sum_{n=0}^{N-1}[X_s(n) - X_r(n)]^2}{N}}, \tag{13}$$

$$SNR(dB) = 10 \times \log\left(\frac{\sum_{n=0}^{N-1}[X_s(n) - X_m]^2}{\sum_{n=0}^{N-1}[X_s(n) - X_r(n)]^2}\right), \tag{14}$$

$$QS = \frac{CR}{PRD}, \tag{15}$$

where Xs(n) represents the original signal; Xr(n) represents the reconstructed signal, and Xm represents the average of Xs(n). Note that the quality score (QS) parameter denotes the ratio of a CR value to a PRD value, which is given by (15). In general, the larger the CR value, the better; the smaller the PRD value, the better. Higher QS represents a better compression rate and lower signal distortion. In this paper, we use QS as another key parameter applied to fairly evaluate the performance of various compression algorithms. For these test patterns, each record from the MIT-BIH database contains two leads, and it should be noticed that each lead has 650,000 units of data. We convert the amplitude of each unit of data into a 16-bit format as in Lee *et al.* [18], and the proposed compression algorithm programmed using MATLAB software is then executed. To obtain the minimum distortion for this lossy compression, we only adopted the 100% window size [18] to develop the proposed algorithm.

Table II lists various performance metrics of the proposed method with all 48 lead-II patterns from the MIT-BIH database, respectively. The CR, PRD, PRDN, RMS, SNR, and QS averages are 6.86, 0.18, 2.60, 1.68, 32.19, and 39.86, respectively.

Table III shows the analytic performance results for various related works and the proposed algorithm. The CR value of the proposed algorithm is higher than that of Lee *et al.*'s method [18]. Additionally, the proposed algorithm has the lowest PRD value and the highest SNR value. These results clearly show that the proposed compression algorithm has the advantages of high accuracy and a high compression rate, so it can obtain a very high quality score of more than 39. Compared with Lee *et al.*'s algorithm, the QS value of the proposed method is greatly increased by 76%. This also implies that the proposed algorithm would be a better solution if employed on a portable device or a system in e-health care, as it requires much less power consumption, especially in data transmission.

VI. Conclusions

In this paper a bio-potential conductive snap is successfully applied to an FPDE by using MEMS technology. It increases sensing stability and is comfortable for long-term use. The proposed FPDE fabrication process shown in this work provides a stable method that can be used to define a metal pattern on a PDMS substrate, and the FPDE can clearly acquire ECG signals with skin touch. Additionally, a new compression concept based on a DCT-IV computation, which is different from the traditional DCT-II-based compression algorithm, is proposed to achieve higher CR and QS than other approaches. We also designed a compact, smaller DCT-IV accelerator on the Altera DE0-Nano FPGA platform, and it uses fewer hardware resources in implementation. Overall, the method presented in this work is very suitable for prototype design of portable personal health monitoring devices.

Acknowledgment

The authors would like to thank the National Nano Device Laboratories (NDL), Taiwan, for supporting the sensor fabrication service.

References

[1] P. Griss, P. Enoksson, H. K. Tolvanen-Laakso, P. Meriläinen, S. Ollmar, and G. Stemme, "Micromachined electrodes for biopotential measurements physiological signal measurements," *J. Microelectromech. Syst.*, vol. 10, no. 1, pp. 10–16, Mar. 2001.

[2] P. Griss, H. K. Tolvanen-Laakso, P. Merilainen, and G. Stemme, "Characterization of micromachined spiked biopotential electrodes," *IEEE Trans. Biomed. Eng.*, vol. 49, no. 6, pp. 597–604, Jun. 2002.

[3] P. Griss, P. Enoksson, and G. Stemme, "Micromachined barbed spikes for mechanical chip attachment," *Sens. Actuators A, Phys.*, vol. 95, nos. 2–3, pp. 94–99, Jan. 2002.

[4] L. M. Yu, F. E. H. Tay, D. G. Guo, L. Xu, and K. L. Yap, "A microfabricated electrode with hollow microneedles for ECG measurement," *Sens. Actuators A, Phys.*, vol. 151, no. 1, pp. 17–22, Apr. 2009.

[5] M. Matteucci *et al.*, "Micropatterned dry electrodes for brain–computer interface," *Microelectron. Eng.*, vol. 84, nos. 5–8, pp. 1737–1740, May/Aug. 2007.

[6] C.-L. Chang, C.-W. Chang, C.-M. Hsu, C.-H. Luo, and J.-C. Chiou, "Power-efficient wireless sensor for physiological signal acquisition," *J. Micro/Nanolithography, MEMS MOEMS*, vol. 8, no. 2, p. 021120, Apr./Jun. 2009.

[7] C.-L. Chang *et al.*, "A power-efficient bio-potential acquisition device with DS-MDE sensors for long-term healthcare monitoring applications," *Sensors*, vol. 10, no. 5, pp. 4777–4793, May 2010.

[8] A. Gruetzmann, S. Hansen, and J. Müller, "Novel dry electrodes for ECG monitoring," *Physiol. Meas.*, vol. 28, no. 11, pp. 1375–1390, 2007.

[9] J.-Y. Baek, J.-H. An, J.-M. Choi, K.-S. Park, and S.-H. Lee, "Flexible polymeric dry electrodes for the long-term monitoring of ECG," *Sens. Actuators A, Phys.*, vol. 143, no. 2, pp. 423–429, 2008.

[10] E. Nemati, M. J. Deen, and T. Mondal, "A wireless wearable ECG sensor for long-term applications," *IEEE Commun. Mag.*, vol. 50, no. 1, pp. 36–43, Jan. 2012.

[11] W.-S. Wang *et al.*, "Wireless biopotential acquisition system for portable healthcare monitoring," *J. Med. Eng. Technol.*, vol. 35, no. 5, pp. 254–261, May 2011.

[12] H. Y. Gan, P. K. Gopalakrishnan, T. H. Teo, and Z. Chen, "A low-complexity ultra-low-power ECG compression and transmission scheme," in *Proc. 12th Int. Symp. Integr. Circuits (ISIC)*, Dec. 2009, pp. 683–686.

[13] S.-L. Chen, H.-Y. Lee, C.-A. Chen, H.-Y. Huang, and C.-H. Luo, "Wireless body sensor network with adaptive low-power design for biometrics and healthcare applications," *IEEE Syst. J.*, vol. 3, no. 4, pp. 398–409, Dec. 2009.

[14] K. Ranjeet, A. Kumar, and R. K. Pandey, "ECG signal compression using different techniques," in *Proc. Int. Conf. Adv. Commun. Comput. Control*, vol. 125, Jan. 2011, pp. 231–241.

[15] L. V. Batista, E. U. K. Melcher, and L. C. Carvalho, "Compression of ECG signals by optimized quantization of discrete cosine transform coefficients," *Med. Eng. Phys.*, vol. 23, no. 2, pp. 127–134, Mar. 2001.

[16] M. S. Alam and N. M. S. Rahim, "Compression of ECG signal based on its deviation from a reference signal using discrete cosine transform," in *Proc. IEEE Elect. Comput. Eng. (ICECE)*, Dec. 2009, pp. 53–58.

[17] S. Lee and M. Lee, "A real-time ECG data compression algorithm for a digital holter system," in *Proc. 30th Annu. Int. IEEE EMBS Conf.*, Aug. 2008, pp. 4736–4739.

[18] S. Lee, J. Kim, and M. Lee, "A real-time ECG data compression and transmission algorithm for an e-health device," *IEEE Trans. Biomed. Eng.*, vol. 58, no. 9, pp. 2448–2455, Sep. 2011.

[19] A. Bendifallah, R. Benzid, and M. Boulemden, "Improved ECG compression method using discrete cosine transform," *Electron. Lett.*, vol. 47, no. 2, pp. 87–89, Jan. 2011.

[20] H.-L. Chan, Y.-C. Chiu, Y.-A. Kao, and C.-L. Wang, "VLSI implementation of wavelet-based electrocardiogram compression and decompression," *J. Med. Biol. Eng.*, vol. 31, no. 5, pp. 331–338, Jul. 2010.

[21] S. K. Mukhopadhyay, M. Mitra, and S. Mitra, "An ECG data compression method via R-peak detection and ASCII character encoding," in *Proc. Int. Conf. Comput., Commun. Elect. Technol. (ICCCET)*, Mar. 2011, pp. 136–141.

[22] S. K. Mukhopadhyay, M. Mitra, and S. Mitra, "A lossless ECG data compression technique using ASCII character encoding," *Comput. Elect. Eng.*, vol. 37, no. 4, pp. 486–497, Jul. 2011.

[23] J. Istle, P. Mandelbaum, and E. Regentova, "Online compression of ASCII files," in *Proc. Int. Conf. Inf. Technol., Coding Comput. (ITCC)*, vol. 1, Apr. 2004, pp. 755–759.

[24] S.-C. Lai, W.-C. Chien, C.-S. Lan, M.-K. Lee, C.-H. Luo, and S.-F. Lei, "An efficient DCT-IV-based ECG compression algorithm and its hardware accelerator design," in *Proc. Int. Symp. Circuits Syst. (ISCAS)*, May 2013, pp. 1296–1299.

[25] *JPEG Entropy Coding*, accessed on Jul. 10, 2016. [Online]. Available: http://cnx.org/content/m11096/latest/

[26] *MIT-BIH Arrhythmia Database*, accessed on Jul. 10, 2016. [Online]. Available: http://www.physionet.org/physiobank/database/mitdb/

[27] S.-C. Lai, S.-F. Lei, and C.-H. Luo, "Common architecture design of novel recursive MDCT and IMDCT algorithms for application to AAC, AAC in DRM, and MP3 codecs," *IEEE Trans. Circuits Syst. II, Exp. Briefs*, vol. 56, no. 10, pp. 793–797, Oct. 2009.

[28] S.-C. Lai, Y.-P. Yeh, W.-C. Tseng, and S.-F. Lei, "Low-cost and high-accuracy design of fast recursive MDCT/MDST/IMDCT/IMDST algorithms and their realization," *IEEE Trans. Circuits Syst. II, Exp. Briefs*, vol. 59, no. 1, pp. 65–69, Jan. 2012.

[29] J. Y. Baek *et al.*, "Stable deposition and patterning of metal layers on the PDMS substrate and characterization for the development of the flexible and implantable micro electrode," *Solid State Phenomena*, vols. 124–126, pp. 165–168, Jun. 2007.

[30] *Agilent E4980A Precision LCR Meter Analyzer Programming Manual*, Agilent, Santa Clara, CA, USA, 2011.

[31] A. Karilainen, S. Hansen, and J. Müller, "Dry and capacitive electrodes for long-term ECG-monitoring," in *Proc. 8th Annu. Workshop Semiconductor Adv. Future Electron.*, 2005, pp. 155–161.

[32] D.-H. Kim *et al.*, "Epidermal electronics," *Science*, vol. 333, no. 6044, pp. 838–843, 2011.

[33] J.-H. Moon, D. H. Baek, Y. Y. Choi, K. H. Lee, H. C. Kim, and S.-H. Lee, "Wearable polyimide–PDMS electrodes for intrabody communication," *J. Micromech. Microeng.*, vol. 20, no. 2, pp. 25–32, 2010.

Ching-Hsing Luo received the B.S. degree in electrophysics from National Chaio Tung University, Hsinchu, Taiwan, the M.S. degree in electrical engineering from National Taiwan University in 1982, the M.S. degree in biomedical engineering from Johns Hopkins University, Baltimore, MD, USA, in 1987, and the Ph.D. degree in biomedical engineering from Case Western Reserve University, Cleveland, OH, USA, in 1991. He has been a Full Professor with the Department of Electrical Engineering, National Cheng Kung University, Tainan, Taiwan, since 1996 and was honored as a Distinguished Professor in 2005. His research interests include biomedical instrumentation-on-a-chip, assistive tool implementation, cell modeling, signal processing, home automata, RFIC, gene chips, and pulse diagnosis platform in traditional Chinese medicine.

Wei-Jhe Ma was born in Taipei, Taiwan, in 1987. He received the B.S. degree in electronic engineering from the National Taipei University of Technology, Taiwan, in 2009, and the M.S. degree in electrical engineering from National Cheng Kung University in 2011. He is currently pursuing the Ph.D. degree with the Department of Electrical Engineering, National Cheng Kung University. He is a member of the Chinese Western Medical Instrument Chip System Laboratory, National Cheng Kung University. His research field includes bio-electrochemical signal acquisition and system design, biomedical system device, biotelemetry system, and analog IC design.

Wen-Ho Juang was born in Taiwan. He received the M.S. degree from the Department of Electrical Engineering, National Cheng Kung University, Tainan, Taiwan, in 2010. From 2011 to 2014, he was an Engineer with the Data Center Networking BU, MediaTek Inc., Hsinchu, Taiwan. He is currently pursuing the Ph.D. degree with the Department of Electrical Engineering, National Cheng Kung University, Tainan, Taiwan. His research interests include digital signal processing and VLSI system design.

Shin-Hung Kuo was born in Tainan, Taiwan, in 1984. He received the B.S. and M.S. degrees from the Department of Electrical Engineering, National Cheng Kung University, Taiwan, in 2007 and 2009, respectively. He is currently pursuring the Ph.D. degree with the Department of Electrical Engineering, National Cheng Kung University. His research interests have been mainly focused on biosensor, microfluidic, and MEMS technology for biomedical applications.

Chih-Yuan Chen was born in Taipei, Taiwan, in 1985. He received the B.S. degree from the Department of Electrical Engineering, National Formosa University, Taiwan, in 2007 and the M.S. degree from the Institute of Nanotechnology and Microsystems Engineering, National Cheng Kung University in 2008. He is currently pursuing the Ph.D. degree with the Department of Electrical Engineering, National Cheng Kung University. His research has been mainly focused on bio-sensing, microfluidic, MEMS technology, and biosensor for physical signal applications.

Pei-Chen Tai was born in Changhua, Taiwan. She received the M.S. degree from the Department of Electrical Engineering, National Cheng Kung University, Tainan, Taiwan, in 2012. Her research interests include digital signal processing, data compression algorithm, and embedded system application.

Shin-Chi Lai was born in Taichung, Taiwan, in 1980. He received the B.S. degree in electronics engineering from ChienKuo Technology University, Changhua, Taiwan, in 2002, the M.S. degree in electronic engineering from the National Yunlin University of Science and Technology, Yunlin, Taiwan, in 2005, and the Ph.D. degree from National Cheng Kung University, Tainan, Taiwan, in 2011. From 2011 to 2013, he had been an Assistant Research Fellow with the Department of Electrical Engineering, National Cheng Kung University, Tainan, Taiwan. Since 2013, he has been an Assistant Professor with the Department of Computer Science and Information Engineering, Nanhua University, Chiayi, Taiwan. His main research interests are in digital signal processing and its circuit design, especially for speech, audio, biomedical, and multimedia applications.